Journal of Materials Research and Technology 27 (2023) 5854–5867

Contents lists available at ScienceDirect

Journal of Materials Research and Technology

journal homepage: www.elsevier.com/locate/jmrt

Homogeneity, metallurgical, mechanical, wear, and corrosion behavior of Ni and B_4C coatings deposited on 304 stainless steels developed by microwave cladding technique

Shashi Prakash Dwivedi [a,**], Shubham Sharma [b,c,d,*], Arun Pratap Srivastava [a], Vandana Arora Sethi [e], Kahtan A. Mohammed [f,g], Abhinav Kumar [h], M. Ijaz Khan [d,i], Mohamed Abbas [j], Elsayed M. Tag-Eldin [k,***]

[a] Lloyd Institute of Engineering & Technology, Plot No. 3, Knowledge Park II, Greater Noida, Uttar Pradesh 201306, India
[b] Mechanical Engineering Department, University Centre for Research and Development, Chandigarh University, Mohali, Punjab, 140413, India
[c] School of Mechanical and Automotive Engineering, Qingdao University of Technology, 266520, Qingdao, China
[d] Department of Mechanical Engineering, Lebanese American University, Kraytem 1102-2801, Beirut, Lebanon
[e] Lloyd Institute of Management and Technology, Plot No 11, Knowledge Park II, Greater Noida, Uttar Pradesh 201306, India
[f] Faculty of Pharmacy, Jabir Ibn Hayyan Medical University, Najaf, Iraq
[g] Department of Medical Physics, Hilla University College, Babylon, Iraq
[h] Department of Nuclear and Renewable Energy, Ural Federal University Named After the First President of Russia, Boris Yeltsin, 19 Mira Street, 620002, Ekaterinburg, Russia
[i] Department of Mechanics and Engineering Science, Peking University, Beijing 100871, China
[j] Electrical Engineering Department, College of Engineering, King Khalid University, Abha 61421, Saudi Arabia
[k] Faculty of Engineering, Future University in Egypt, 11835 Cairo, Egypt

ARTICLE INFO

Handling Editor: L Murr

Keywords:
Microwave cladding
Interfacial bond layer
Number of grains
Hardness
Corrosion
Wear

ABSTRACT

The microwave cladding technique for depositing Ni and 10 % B_4C coatings on 304 stainless steel has yielded significant advancements in material properties and performance. The key findings of this study revealed remarkable improvements, including a 43.33% increase in material hardness, indicating enhanced wear resistance and mechanical properties. This improvement was attributed to the uniform distribution of B_4C and Ni on the cladding surface, ensuring a consistent interfacial layer developed between SS 304 and the cladding surface without cracks and porosity. Microstructural analysis at 500× magnification unveiled an impressive 2233.35 grains per square inch, showcasing the refined grain structure achieved during the cladding process. Wear testing demonstrated a low wear rate of 0.00308 mm^3/m and a favorable coefficient of friction of 0.1981, confirming the material's suitability for applications with demanding frictional conditions. Furthermore, the corrosion behavior of the coated 304 stainless steel was assessed, revealing a minimal corrosion weight loss of only 0.42 mg for the Ni and 10% B_4C coated sample. The presence of various carbide phases, such as Cr_2C, $Cr_{23}C_6$, Cr_7BC_4, Fe_5C_2, and $Fe_{23}B_6$, within the cladding further contributed to the material's enhanced mechanical and wear properties.

1. Introduction

Steel is one of the most widely used materials in the world due to its exceptional strength and durability. Steel is a ubiquitous material in modern industry, and can be significantly enhanced through the incorporation of various ceramic particles as coatings [1]. This innovative approach combines the strength and malleability of steel with the exceptional properties of ceramics, opening up a wide range of applications across different sectors [2,3]. One common ceramic material used for steel coating is alumina (Al_2O3). Alumina coatings are prized

* Corresponding author. Lloyd Institute of Engineering & Technology, Plot No. 3, Knowledge Park II, Greater Noida, Uttar Pradesh 201306, India.
** Corresponding author.
*** Corresponding author.
E-mail addresses: spdglb@gmail.com (S.P. Dwivedi), shubham543sharma@gmail.com, shubhamsharmacsirclri@gmail.com (S. Sharma), Elsayed.tageldin@fue.edu.eg (E.M. Tag-Eldin).

https://doi.org/10.1016/j.jmrt.2023.10.202
Received 30 August 2023; Accepted 19 October 2023
Available online 7 November 2023

for their excellent hardness, wear resistance, and corrosion resistance [4]. When applied to steel surfaces, they form a protective layer that shields against abrasive wear, extending the lifespan of components in heavy machinery and cutting tools. Another notable ceramic coating is zirconia (ZrO_2). Zirconia-coated steel exhibits superior thermal and chemical resistance, making it suitable for applications in high-temperature environments such as gas turbines and industrial furnaces [5,6]. Zirconia coatings can also enhance the electrical insulation properties of steel, a valuable feature for electronic and electrical applications. Additionally, silicon carbide (SiC) coatings are known for their extreme hardness and abrasion resistance [7,8]. When combined with steel, SiC coatings find applications in armor protection, cutting tools, and high-performance bearings [9–12]. Titanium nitride (TiN) coatings are popular for their gold-like appearance and excellent wear resistance. They are often used on steel tools and components in the automotive and aerospace industries [13–15].

Boron carbide (B_4C) is a versatile material used in various industrial applications, including its utilization as a coating for steel surfaces [16]. This ceramic compound offers several advantages in enhancing the performance and durability of steel components. First and foremost, B_4C coatings are renowned for their exceptional hardness [17]. This property makes them highly resistant to abrasion, wear, and scratches, which is particularly beneficial for steel used in harsh environments or subjected to heavy mechanical stress [18–20]. Moreover, B4C coatings provide excellent corrosion resistance. Steel is susceptible to rust and degradation when exposed to moisture and corrosive substances, but a B_4C coating acts as a protective barrier, extending the lifespan of the steel component [21–23]. Additionally, B_4C-coated steel can exhibit improved thermal stability and electrical conductivity, making it suitable for applications in high-temperature environments and electronic industries [24–26].

The combination of nickel (Ni) with boron carbide (B_4C) for steel coating offers a unique set of advantages in terms of enhancing the performance and properties of steel components [27,28]. This composite coating is particularly valuable in demanding industrial applications. Nickel, known for its excellent corrosion resistance and electrical conductivity, provides a robust protective layer when combined with B_4C. B_4C is exceptionally hard and wear-resistant, making it ideal for guarding steel against abrasive wear and scratches [29,30]. The synergy between Ni and B_4C in a coating improves the overall hardness, wear resistance, and corrosion resistance of the steel substrate [31,32]. This, in turn, extends the lifespan of steel components, reduces maintenance costs, and enhances their performance in harsh environments. Additionally, the electrical conductivity of nickel allows for specific applications where electrical or thermal conductivity is crucial.

Traditional cladding techniques, although effective in many applications, come with several inherent problems that have driven the exploration of alternative methods like microwave cladding. Traditional cladding methods like welding or thermal spraying can lead to variations in coating thickness, resulting in uneven protection and performance [33,34]. Welding processes often introduce HAZ, altering the mechanical properties of the substrate and creating potential weak points. Some cladding materials are incompatible with certain substrates, limiting material choices and applications. Conventional cladding methods can be energy-intensive, leading to higher operational costs and environmental concerns. Thermal spraying and similar methods may have relatively slow deposition rates, impacting productivity. Material waste is common in traditional cladding processes due to overspray, spatter, or excessive heat [35,36]. Microwave cladding offers a potential solution to the traditional cladding problems. Microwave cladding allows for precise control of temperature distribution, leading to uniform coating thickness and properties across the substrate. Microwave cladding operates at lower temperatures, reducing the likelihood of heat-affected zones and substrate property alterations. Microwave cladding can be applied to a wide range of materials and substrates, enhancing compatibility and expanding applications. Microwave heating is efficient and can significantly reduce energy consumption compared to traditional methods. Microwave cladding can achieve rapid heating and deposition, increasing production rates [37]. With precise material distribution, microwave cladding can minimize waste, making it a more cost-effective and environmentally friendly option.

In a study by B. Singh et al. [38], the microwave cladding behavior was reviewed, and it was strongly recommended to employ protective coatings to prevent erosion damage. C. Durga Prasad et al. [39] innovatively created a cladding surface on AISI 410 steel through microwave irradiation, using a combination of CoMoCrSi and Flyash. X-ray diffraction (XRD) analysis unveiled the presence of various hard phases, including Mo_3Si, SiC, TiC, Co_3Ti, and Cr_3C_2. This research demonstrates the effectiveness of microwave-based methods in producing enhanced surface coatings with a combination of hard phases for improved material properties. In their work, B. Singh et al. [40] employed a modified B-type thermocouple to create a Ni-based cladding while simultaneously measuring real-time temperature distribution. This innovative approach allowed for precise monitoring of temperature changes during the cladding process, facilitating better control and understanding of the thermal dynamics involved.

J.S. Vishwanatha et al. [41] successfully developed microwave clads on an AISI 420 substrate within a remarkably short exposure time of just 7 min. Their research revealed significant improvements in erosion resistance for the clad surfaces, surpassing the performance of the original substrates. This achievement highlights the efficacy of microwave cladding in enhancing the material's resistance to erosion, which has implications for various industrial applications requiring improved durability. K. P. Kumar et al. [42] employed nickel microwave cladding to significantly enhance the surface properties of austenitic stainless steel. The cladding process resulted in improved resistance to oxidation and wear, though a thin oxide layer was observed on clad surfaces. Notably, the clad region exhibited a substantially higher microhardness of 458 HV compared to the substrate region's 234 HV. The presence of silicon, cobalt, and chromium in the cladding further contributed to the material's enhanced surface characteristics.

Bhupinder Singh et al. [43] investigated the influence of post-clad heat treatment on Ni-based microwave cladding. Their findings revealed that at 1000 °C, the clad material undergoes partial dissolution of eutectic carbides during heat treatment, shedding light on the thermal transformations occurring within the cladded structure. T. K. Mishra et al. [44] employed microwave hybrid heating to deposit nickel and nickel-tungsten carbide cladding on a low-carbon steel base. The research highlighted that incorporating 12 wt % of tungsten carbide (WC) significantly improved the cladding's resistance to abrasive wear, microstructure, and hardness. Interestingly, the Ni-12 wt% WC coating exhibited greater hardness compared to the Ni-24 wt% WC coating, suggesting an optimal composition for enhanced material properties. A. Babu et al. [45] synthesized Ni–SiC composite claddings, revealing remarkable corrosion resistance, with Ni–SiC bimodal cladding outperforming WCCoCr coating by sevenfold. However, Ni–SiC microwave claddings exhibited a combination of brittle and ductile degradation processes, underscoring the importance of considering both their strengths and limitations in various applications. Rakesh. B. Nair et al. [46] utilized microwave heating to develop AlxCoCrFeNi high entropy alloy claddings. These claddings exhibited impressive erosion resistance, with the equimolar high entropy alloy showing erosion rates nearly 23 times lower than those observed in SS316L steel, emphasizing their potential as superior materials for applications where erosion resistance is critical. Sunny Zafar et al. [47] harnessed microwave radiation to fabricate clads featuring nanostructures, with nano-carbides distributed in a consistent pattern. The produced clads exhibited impressive mechanical properties, boasting a flexural strength averaging 671 ± 28 MPa and a microhardness of 1760 ± 128 HV. This highlights the potential of microwave cladding for engineering materials with enhanced nanostructural features and remarkable mechanical strength.

Ajit M. Hebbale et al. [48] employed microwave irradiation to create a Ni-based coating on austenitic SS-304. Microstructure analysis revealed a remarkably low porosity of approximately 0.87%, while increased hardness was attributed to the dispersion of intermetallics and metal carbides. The resulting clad surface exhibited a notable microhardness, averaging 364 ± 70 HV, showcasing the efficacy of microwave cladding for enhancing material properties and surface hardness.

The research gap in the present study lies in the limited understanding of the comprehensive and synergistic impact of microwave cladding technology on the properties of Ni and B_4C coatings when applied to 304 stainless steels. Despite significant advancements in coating technologies and their applications in various industries, there is a distinct lack of research that investigates the combined effect of microwave cladding, Ni coatings, and B_4C in the context of 304 stainless steel. Existing studies often focus on individual aspects, such as coating material or deposition technique, but fail to address the holistic evaluation of these multifaceted coatings on the specific substrate. This research gap calls for a thorough investigation to bridge the knowledge void and provide valuable insights into the performance of these coatings in a real-world application.

This research aims to address a critical knowledge gap by pioneering a comprehensive study of the homogeneity, metallurgical attributes, mechanical properties, and the wear and corrosion behavior of Ni and B4C coatings when applied to 304 stainless steels using the innovative microwave cladding technique. The novelty of this study lies in its holistic approach, as it integrates multiple factors that have not been studied collectively before. By using the novel microwave cladding method to deposit Ni and B_4C coatings on 304 stainless steels, this research will provide unique insights into the synergistic effects of these coatings, offering a significant advancement in the field of materials science and surface engineering. The objective of this study is to develop and characterize Ni and B_4C-coated SS-304 steel using the microwave cladding technique. The specific aims of the study are to investigate the microstructural and mechanical properties of the coated steel and evaluate the coating's resistance to wear, and corrosion.

2. Materials and methods

2.1. Base material

SS 304 has a face-centered cubic (FCC) crystal structure, which contributes to its excellent mechanical and corrosion-resistant properties. The FCC structure allows for close-packed atomic arrangements, enhancing its strength and ductility. SS 304 has a density of around 8 g/ cm^3, making it moderately dense. Thermal Conductivity: It has a relatively low thermal conductivity of about 16.2 W/(m·K). SS 304 exhibits moderate electrical conductivity. SS 304 is primarily composed of iron, chromium (18–20%), and nickel (8–10.5%). It contains small amounts of carbon ($\leq$0.08%) and manganese ($\leq$2%), which contribute to its corrosion resistance and weldability. The presence of chromium forms a passive oxide layer on the surface, providing excellent corrosion resistance, especially in various corrosive environments [1]. Table 1 displays analyzed the properties of SS-304 up to 160 mm diameter/thickness.

2.2. Primary cladding particle

Fig. 1 shows powder XRD of Ni powder used in the present study. The average particle size of Ni was 18 μm. The application of nickel (Ni) coating on steel substrates, combined with boron carbide (B_4C) reinforcement, using microwave cladding techniques, offers significant enhancements to the material's properties. Ni coating provides several advantages, such as corrosion resistance, increased hardness, and enhanced wear resistance. When B_4C particles are incorporated into the Ni matrix, the resulting composite exhibits exceptional properties, including improved strength and abrasion resistance [27]. The microwave cladding technique allows for a homogenous distribution of B_4C particles within the Ni coating, ensuring superior mechanical and thermal properties. The coating thickness range of Ni with B_4C on steel can vary depending on the specific application and the desired performance characteristics [29]. However, for better surface properties, it is essential to consider a coating thickness range that balances both functionality and cost-effectiveness. Here are some general guidelines.

Table 1
Analyzed the Properties of SS-304 up to 160 mm diameter/thickness [49].

S. No.	Properties	Values
1	Density (g/cm^3)	8
2	Tensile Strength (MPa)	615
3	Melting Temperature (Degree centigrade)	1450
4	Vicker Hardness (HV)	210

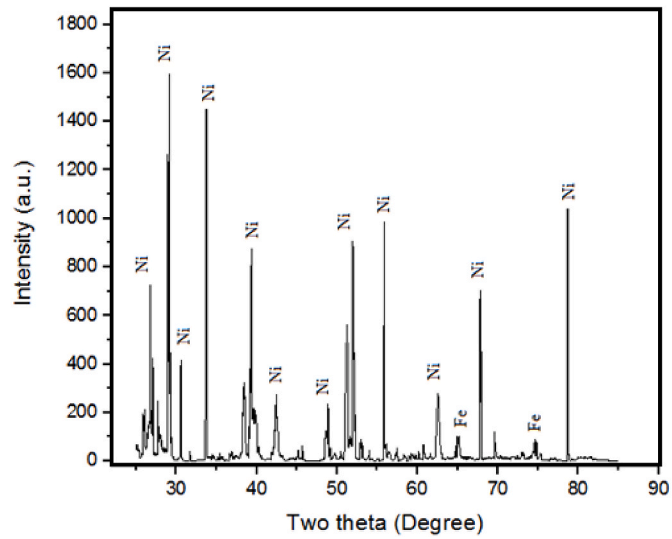

Fig. 1. Powder XRD of Ni powder.

2.2.1. Thin coatings (5–50 μm)

- Thin coatings are suitable for applications where surface enhancement is the primary goal, such as improving wear resistance, corrosion resistance, or surface hardness.
- These coatings are typically cost-effective and may provide good results for applications with moderate wear or corrosion challenges.

2.2.2. Moderate coatings (50–200 μm)

- Moderate coatings strike a balance between cost and performance.
- They are suitable for applications where higher wear resistance or improved surface properties are required, but there are constraints on coating thickness.

2.2.3. Thick coatings (>200 μm)

- Thick coatings are used when extreme wear resistance, extended service life, or severe environmental conditions are expected.
- These coatings may be necessary for heavy-duty industrial equipment or components subjected to aggressive wear and corrosion.

2.3. Secondary cladding particle

Boron carbide (B_4C) with an average particle size of 20 μm was chosen as a secondary reinforcement particle. B_4C is manufactured through various methods, including solid-state reaction processes and chemical vapor deposition (CVD). It is often synthesized from a mixture of boron oxide and carbon-containing precursors at high temperatures. B_4C has a complex crystal structure, primarily consisting of boron (B) and carbon (C) atoms arranged in an icosahedral boron-based lattice. This structure imparts B_4C with remarkable hardness, making it one of the hardest materials known, second only to diamond. B_4C typically consists of approximately 77–80% boron and 20–23% carbon. Its chemical composition makes it resistant to chemical reactions with most acids and bases. B_4C is renowned for its exceptional hardness, high modulus of elasticity, and excellent wear resistance [31]. Fig. 2 is an X-ray powder diffraction pattern of the B_4C particles employed in this investigation. The X-ray powder diffraction pattern of B_4C powder reveals B_4C, B_2O_3, and C phases as illustrated in the Fig. 3.

2.4. Development of cladding

In the present study, an In-house developed microwave oven was used for the cladding process. Microwave hybrid heating was carried out at 900 W with 2.45 GHz frequency (Table 2). Alcohol was used in an ultrasonic bath to clean the SS-304 substrate before deposition. Ni and B_4C particles (10% of the total) were heat treated in a muffle furnace for 24 h at 1100 °C. Ni and 10 % B_4C combination was preheated to drive out any remaining moisture. The warmed powder was sprinkled on the SS-304 substrate in a roughly even layer. Microwave interaction is material-dependent, with a key factor being skin depth, particularly crucial for swift interaction. In the context of hard-facing powder, maintaining the primary ingredient at a 4.5 m skin depth at 2.45 GHz helps avoid direct particle interaction with microwave radiation at ambient temperature, optimizing the cladding process. To mitigate microwave reflection issues caused by a Ni and 10% B4C powder blend clads were fabricated using charcoal as the susceptor material via microwave hybrid heating (MHH). This substitution effectively addresses reflection challenges, ensuring efficient heating and material processing in the MHH method [47,48]. At room temperature, charcoal exhibited strong microwave interaction, resulting in rapid heating. This phenomenon subsequently elevated the temperature of the Ni and 10% B4C powder in the mixture, facilitating effective and efficient processing in the desired application. The experimental conditions for creating the microwave-clad samples from a 10% B_4C and Ni powder on the SS-304 mixture are shown in Table 2. To prevent contamination of the clad, a pure graphite sheet was interposed between the susceptor and the Ni and 10% B4C powder. The MHH process was executed at 900 W and 2.45 GHz using a multimode microwave applicator, ensuring controlled and efficient heating while safeguarding the quality of the final product. The powder layer underwent 120 s of irradiation. Microwave-clad samples were fabricated using a blend of 10% B4C and Ni powder on SS-304, demonstrating the effectiveness of the microwave cladding process for enhancing the material's properties. A uniform cladding surface was obtained by controlling the cladding process parameters. Optimum process parameters were decided to control the uniform cladding surfaces as per the pilot run investigation as shown in Table 2. Randomly, Irradiation time was chosen 100 s, and other parameters were kept constant. The presence of weak spots and gaps between the substrate and cladding surface was detected with 100 s Irradiation time. This suggested that the cladding process had encountered challenges related to material bonding or uniform deposition within the given timeframe. An issue of porosity became evident on the cladding surface during a 150-s microwave cladding process. This occurrence was attributed to the prolonged irradiation, causing excessive heating of the substrate material. The elevated substrate temperature led to increased gas entrapment within the molten cladding material, resulting in porosity. During a 120-s irradiation time in a cladding process, a significant achievement was the attainment of a uniform cladding surface that was entirely free from porosity. This outcome signified the successful control of irradiation time to ensure the even distribution and bonding of the cladding material onto the substrate. The absence of porosity indicated minimal gas entrapment or voids within the cladding layer, enhancing its structural integrity and corrosion resistance. Following the pilot run investigation, an irradiation time of 120 s was deemed optimal for subsequent cladding processes, ensuring the desired results. The same course of action was conducted to decide the other process parameters (Table 2).

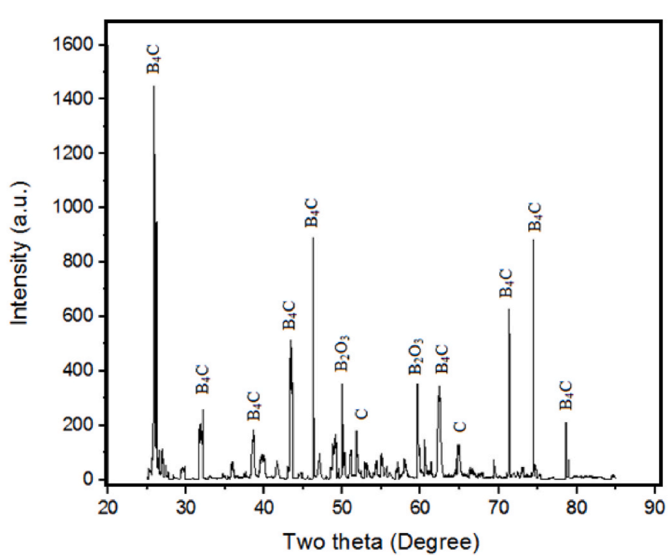

Fig. 2. Powder XRD of B_4C powder.

2.5. Materials testing and equipment

To conduct microstructure analysis, X-ray diffraction (XRD), and hardness measurements on cladding samples of SS 304, you will need specific testing equipment with the following properties [50–55].

2.5.1. Scanning electron microscope (SEM)

- Type: Field-emission SEM (FE-SEM) is used for high-resolution imaging.
- Detector: Secondary Electron (SE) and Backscattered Electron (BSE) detectors for surface imaging and compositional contrast were used.
- Sample stage: Motorized stage for precise sample positioning.
- Chamber: A vacuum environment was used to minimize electron scattering.

2.5.2. X-ray diffraction (XRD) equipment

- XRD type: A powder X-ray diffractometer was used for phase analysis.
- X-ray source: A high-intensity, monochromatic X-ray source (e.g., Cu Kα radiation).
- Detector: A high-resolution, sensitive detector such as a scintillation detector.
- Goniometer: Motorized goniometer for precise sample positioning.
- Sample holder: A sample holder that accommodates cladding samples and enables rotation.

2.5.3. Hardness testing equipment

- Hardness tester: Vickers hardness tester on the hardness scale.
- Load application: Motorized load application system for accurate and consistent loads.

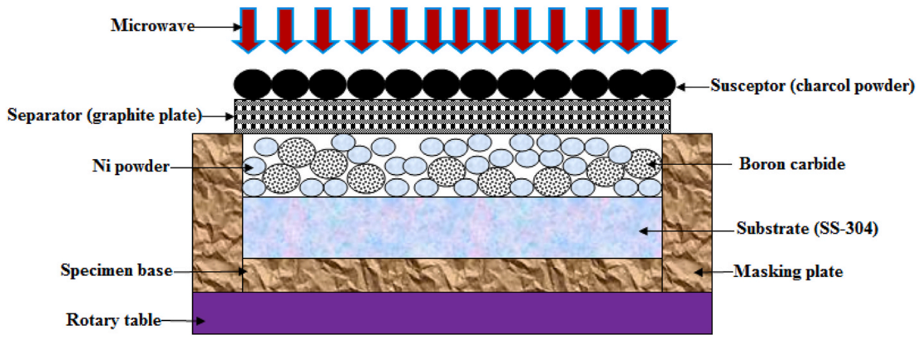

Fig. 3. Experimental procedure.

Table 2
Microwave cladding process parameters [49].

S. No.	Parameters	Description
1	Frequency	2.45 GHz
2	Power	900 W
3	Susceptor	Charcoal
4	Separator	Graphite plate
5	Preheating powder Temperature	120 °C
6	Preheating time of powder	22 h
7	Average cooling time	680 s
8	Irradiation time	120 s
9	Atmosphere	Ambient
10	Powder	Ni + 10 % B_4C
11	Substrate	SS-304

2.6. *Wear testing*

The wear testing procedure on SS 304 steel coated with Ni and 10% B_4C using a pin-on-disc apparatus typically follows these steps [56–58].

2.6.1. *Specimen preparation*

- The SS 304 specimen was prepared with the Ni and 10% B_4C coating.

2.6.2. *Pin-on-disc setup*

- The pin-on-disc test apparatus was set up, consisting of a rotating disc and a fixed pin (counterpart). The disc was made of a material representative of the wear conditions.

2.6.3. *Load and speed configuration*

- A specified load was applied (5 N) on the pin.
- The rotational speed of the disc was set (2 m/s).

2.6.4. *Wear test run*

- The coated SS 304 specimen (pin) was placed in contact with the rotating disc.
- The pin-on-disc apparatus was run for a predetermined distance or time (1000 m).

2.6.5. *Data collection*

- The weight loss of the pin (coated SS 304 specimen) was measured and recorded before and after the test to determine the wear rate.

2.6.6. *Friction measurement*

- The coefficient of friction during the test was monitored and recorded to assess the material's tribological behavior as exhibited in the Fig. 4.

3. Results and discussions

3.1. *Microstructure investigation*

Optical micrographs of clad SS-304 alloy with a 10% B_4C and Ni powder microwave coating are displayed in Fig. 5. Surface areas of SS-304 alloy were able to dissolve Ni powder. However, the steel's surface shows signs of having been contaminated with B_4C powder. In addition to improving the surface quality of steel, Ni powder was also a suitable coating material in and of itself. Introducing a combination of 10% B_4C and nickel (Ni) to steel has yielded remarkable enhancements in surface properties. The most notable improvements lie in heightened hardness and wear resistance. This was largely attributed to the achievement of a uniform distribution of B_4C and Ni (Fig. 6), which resulted in a surface entirely free from porosity and cracks. Such a surface transformation was pivotal in extending the steel's longevity and ensuring it performed exceptionally well in environments characterized by abrasion and wear. The synergy between B_4C and Ni presented a significant advancement in fortifying the steel's surface. However, the structure of a steel sample containing 10% B_4C and Ni gradually shifted from austenite to lower temperature phases as the sample cooled. The change to pearlite and ferrite occurred in the mostly ferritic microstructures of steels (without cladding of B_4C and Ni). The transformation from predominantly ferritic

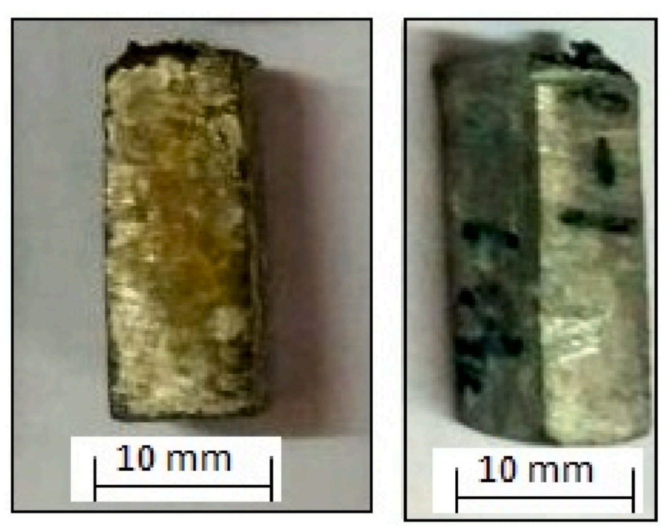

Fig. 4. Photograph of the microwave-clad samples.

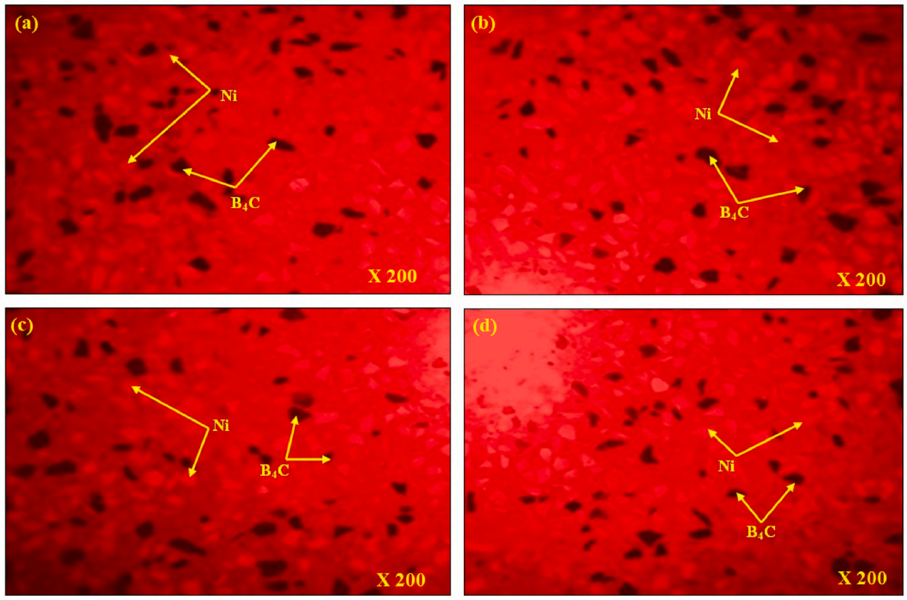

Fig. 5. Optical microscopic images of the cladding surface.

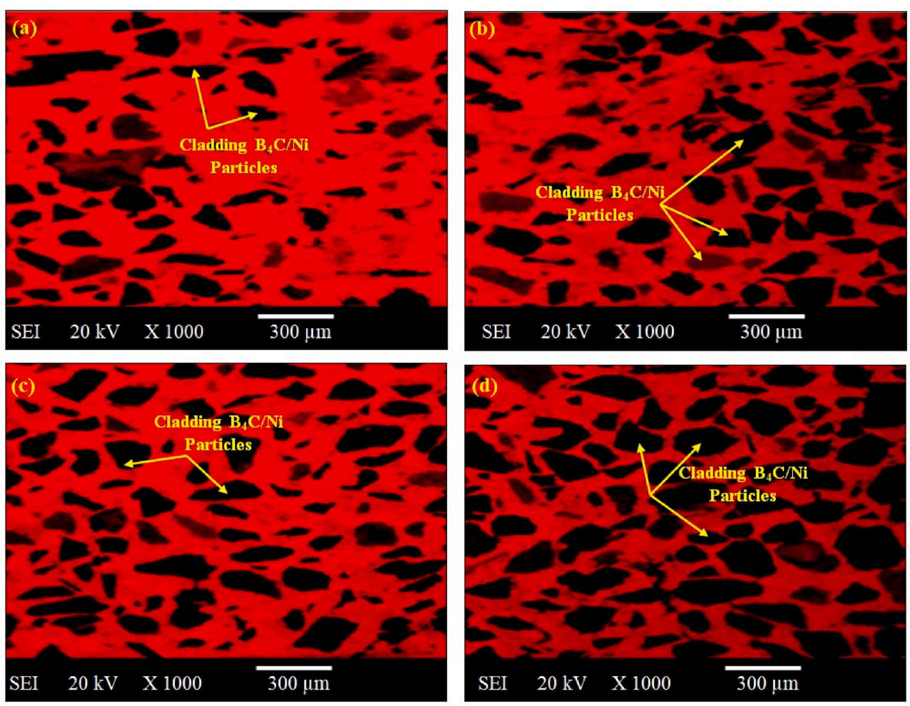

Fig. 6. SEM images of the cladding surface.

microstructures to pearlite and ferrite in steels, without the addition of B_4C (boron carbide) and Ni (nickel) cladding, signified a crucial metallurgical alteration. This transition was achieved due to the effect of heat treatment occurred during the processing, which involved heating and cooling the steel. It resulted in a more balanced microstructure. The presence of pearlite, a lamellar mixture of cementite and ferrite, enhanced hardness and strength, while ferrite contributed to ductility [59,60]. Since interlamellar spacing and the pearlite did not contribute noticeably to the strength of cladding compositions, ferrite grain size was the most essential parameter of concern in this study following microwave cladding of 10% B_4C and Ni on steel. There was evidence that during the solidification phase following microwave processing, ferrite grains of cladding samples nucleated near austenite grain boundaries. It has been noted, however, that the residual strain and the ultimate austenite grain size influenced the ferrite grain size of coated steel. The retained strain and the ultimate austenite grain size were both affected by environmental factors such as cooling rate, composition, and deformation history. After undergoing microwave processing, the austenite grains in the cladding samples grew larger to reach their ultimate, completely recrystallized size [61,62]. The cladding surface and layer were seen in detail in the SEM picture shown in Fig. 7. There were fewer black pixels in the homogeneous cladding layer, as seen in Fig. 7(a & b) (yields a higher homogeneity). An even layer of coating of Ni and B_4C ensured that the substrate was adequately protected [63–65]. The

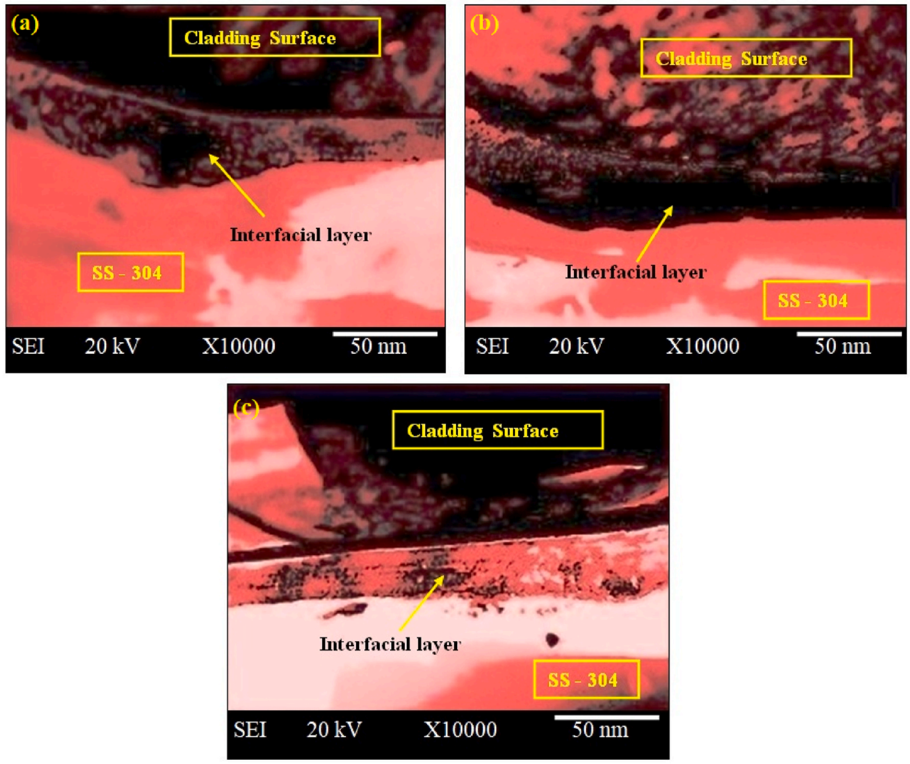

Fig. 7. SEM image of cladding layer and cladding surface.

uniform cladding layer ensured that there were no weak spots or gaps that could expose the substrate to harmful elements [66,67]. Uniform cladding surfaces increased the surface area available for adhesion, improving the bonding strength of the coating [68]. This helped to increase the lifespan of the coated product [56,57]. A uniform and consistent cladding layer enhanced the appearance of the coated surface. It provided a smooth and even surface that added to the overall visual appeal of the product [69–71].

The grain count of SS-304 alloy microwave cladding with a 10% B_4C and Ni powder blend, was determined per square inch at 500× magnification. This analysis provided insights into the microstructural changes induced by the cladding process, offering valuable information about material properties and performance [55,72,73]. The number of grains (n) was observed by following Equation (1):

$$n = 2^{(G-1)} \tag{1}$$

Where, n = the number of grains,
G = grain size number ASTM.

$$G = [-6.644\log_{10}(l_\alpha)] - 3.28 \tag{2}$$

Where, $l_\alpha = \frac{V_{v\alpha}(L_T)}{N_\alpha}$.

Here, $V_{v\alpha}$ = fraction of α phase (volume), L_T = length/magnification (test line), N_α = grains intercepted (number).

Now,

$$l_\alpha = \frac{0.47 \times (493/500)}{95}$$

$$l_\alpha = 0.0048$$

Now again G from Equation (2),

$$G = [-6.644\log_{10}(0.0048)] - 3.28$$

G = 12.125.

Now from Equation (1)

$$n = 2^{(12.125-1)}$$

$$n = 2^{(11.125)}$$

$$n = 2233.35$$

In the examination of SS-304 alloy after microwave cladding with a 10% B_4C and Ni powder blend, a significant finding emerged: approximately 2233.35 grains were observed per square inch at 500× magnification. This numerical insight sheds light on the microstructural transformations resulting from the cladding process [55,74–76]. The rise in grain count signified that the microwave cladding had induced a finer grain structure in the material, which often led to enhanced mechanical characteristics, such as enhanced hardness and wear resistance [77–79].

3.2. XRD behavior

The XRD of a 10% B_4C and Ni powder-clad SS-304 alloy is shown in Fig. 8. X-ray diffraction analysis of a cladding surface reveals the presence of Cr_2C (38.94°, 48.46°, 51.82°, 66.68°, 67.92°, 74.76°), $Cr_{23}C_6$ (34.3°, 42.92°), Cr_7BC_4 (29.32°), Fe_5C_2 (25.94°, 39.06°, 78.96°), and $Fe_{23}B_6$ (45.7°) phases. After being clad with a combination of 10% B_4C and Ni powder, SS-304 alloy gained increased hardness due to the formation of hard and carbide phases such as Cr_2C, $Cr_{23}C_6$, and Cr_7BC_4. Cr_2C (carbide phase) was formed due to the presence of chromium in the steel [80–82]. It provided excellent wear resistance [83,84]. However, excessive carbide formation led to brittleness and reduced the ductility of steel. $Cr_{23}C_6$ was another chromium carbide phase that formed at high temperatures [85–87]. It had a similar effect on steel as Cr_2C, but it was more stable and could provide better corrosion resistance. Cr_7BC_4 (boride phase) was formed by the addition of boron to steel [88–90]. It improved the hardness and wear resistance of steel. The Fe_5C_2 carbide phase was formed by the reaction between iron and carbon [91–94]. It provided hardness and wear resistance to steel. The $Fe_{23}B_6$ boride phase

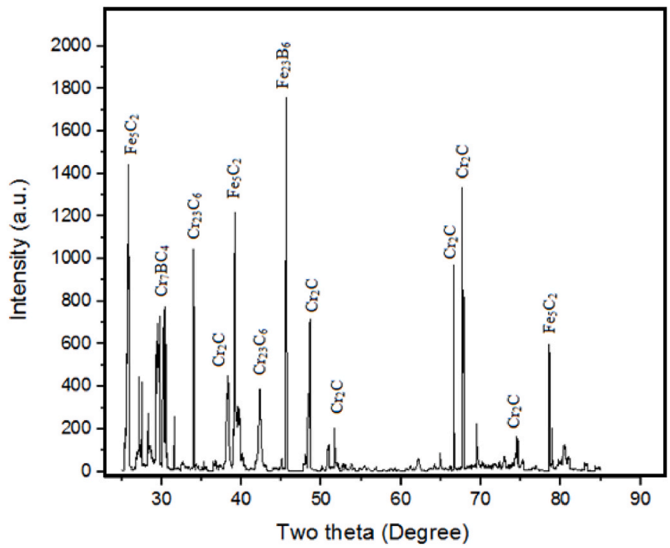

Fig. 8. XRD of SS-304 alloy with the microwave cladding of the mixture of 10 % B_4C and Ni powder.

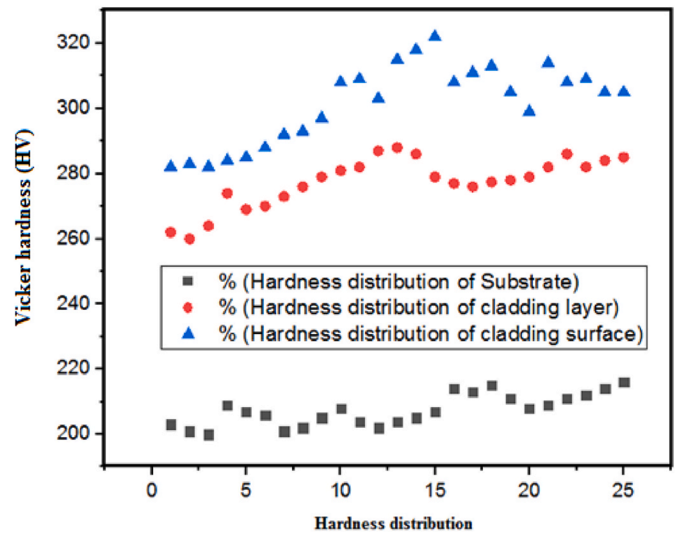

Fig. 9. Hardness distribution from SS-304 to cladding surface.

was formed by the addition of boron to steel. It improved the strength and ductility of steel [95–97].

3.3. Surface hardness

The hardness of SS-304 alloy, after microwave cladding with a 10% B4C and Ni powder blend, plays a pivotal role in defining its surface characteristics. The standard deviation of Vickers hardness readings was within 1–2 HV units in the present study. The SS-304 alloy, originally possessing an average hardness of 210 HV, underwent a transformative change after microwave cladding with a Ni and 10% B_4C powder blend. The resulting cladding surface exhibited a remarkable hardness of approximately 301 HV. This substantial increase of 43.33% in hardness showed a significant enhancement in material properties achieved through the cladding process [98–100]. The elevated hardness indicated improved resistance to wear, abrasion, and deformation, making SS-304 alloy with Ni and 10% B_4C an ideal choice for applications demanding heightened surface durability and performance, such as in the aerospace and manufacturing industries [101–103]. The formation of carbide phases like Cr_2C, $Cr_{23}C_6$, and Cr_7BC_4 during microwave cladding played a pivotal role in boosting material hardness. These carbides contributed to the improved surface properties, providing superior wear resistance and increased durability [104–106]. The generation of these hard phases on the surface contributed to an increase in the resistance of the material to indentation [56,57], hence elevating the hardness of the cladding surface. In Fig. 9, hardness distributions for SS-304, the cladding layer, and the cladding surface were examined. Interestingly, the cladding layer and the cladding surface displayed uniform hardness distributions, indicative of consistent material properties [107–109]. Conversely, SS-304 exhibited significant hardness variability after solidification, suggesting irregularities in its microstructure [58,59]. Notably, the cladding layer exhibited slightly lower hardness when compared to the cladding surface [110,111]. This differential hardness profile reflected the influence of the microwave cladding process, which imparted distinct characteristics to each region.

3.4. Wear behavior

A wear test on the cladding surface of SS-304 with a coating mixture of Ni and 10% B_4C was conducted to assess its performance and durability. In the wear test, a pin-on-disc machine operated at a sliding speed of 2 m/s, traversing a distance of 1000 m while applying an axial load of 5 N. The cladding surface, comprising Ni and 10% B4C, displayed impressive performance attributes, featuring a low wear rate of 0.00308 mm^3/m and a coefficient of friction measuring 0.1981. These results signified its exceptional wear resistance and frictional properties [112–114]. The exceptional wear resistance of the SS 304 cladding can be primarily attributed to the strategic incorporation of B_4C with Ni powder during the cladding process. The addition of B_4C, known for its remarkable hardness and abrasive properties, into the Ni matrix created a composite material that was significantly harder and more wear-resistant than the base SS 304 alloy [115–117]. When SS-304 was coated with the mixture of Ni and 10% B_4C subjected to wear test, the B_4C particles acted as abrasive reinforcements, reducing material loss and minimizing wear [118,119]. Additionally, the composite's microstructure, including fine grains and uniform distribution of B_4C, enhanced its ability to withstand friction and stress [120,121]. This synergistic effect between the constituents enhanced the material's ability to withstand friction, abrasion, and wear [2]. However, the boron carbide (B_4C) was indeed a crucial component known for enhancing a material's resistance to wear. However, sometimes in the context of dynamic stress, certain challenges arise. Cavitation erosion occurred at the interface between the cladding and the SS-304 substrate, leading to the degradation of the Ni-and-10%-B_4C cladding [122–124]. The degradation mechanisms involved multiple factors. Columnar grains within the cladding sheared, leading to damage. Additionally, plastic deformation occurred within the SS-304 substrate due to the stress, further contributing to wear. Undulations and cyclic strain in the substrate led to cladding delamination [125–127]. The elastic nature of the cladding and transient loading caused it to separate from the substrate. In cases of cladding delamination due to cyclic dynamic loads, shear fractures propagated across the entire cladding thickness, resulting in cladding loss [55,58]. Furthermore, cladding undulations induced tensile stresses within the coating, further exacerbating the issue. These stresses initiated and propagated cracks, ultimately impacting the material's overall integrity [128–130]. The microwave cladding of a 10% B_4C and Ni powder blend not only enhanced the wear resistance of SS-304 but also introduced phases like Cr_2C, $Cr_{23}C_6$, and Cr_7BC_4. These newly formed carbide phases significantly contributed to the improved wear behavior of the material [131–133].

In this study, the cladding of Ni and 10% B_4C on SS 304 induced grain refinement, leading to smaller grain sizes. Fine-grained materials had more grain boundaries, which acted as barriers to dislocation movement during wear [134–136]. This helped distribute stress and reduced the propensity for plastic deformation and wear. During wear, particles and wear debris were generated at the contact interface

[137–139]. The incorporation of B_4C in the cladding introduced hard particles with a solid lubricating effect. These particles reduced friction and abrasive wear by forming a protective layer on the contact surfaces [140,141]. The hard B_4C particles withstood abrasive forces, helping to minimize wear. Adhesive wear occurs when surfaces bonded and then separated, leading to material transfer between contacting surfaces [142–144]. The hardness and lubricating effect of the Ni and B_4C coating reduced adhesion by inhibiting material transfer. This helped prevent excessive wear and damage to the underlying material. Grooves were formed on the surface due to abrasive wear. The presence of hard B_4C particles contributed to groove formation as they abraded the surface (Fig. 10).

The wear mechanism and microstructural changes induced by cladding SS 304 with Ni and 10% B_4C were of paramount importance in understanding the material's performance. The hard B_4C particles dispersed within the Ni matrix substantially enhance wear resistance [145,146]. During wear, these hard particles acted as abrasion-resistant reinforcements, effectively reducing material loss due to abrasive contact. Additionally, the cladding process induced microstructural alterations such as grain refinement, dispersion of B_4C, and possibly phase transformations, which collectively contributed to improved wear resistance [147–149]. The wear surface morphology of SS 304 steel coating with Ni and B_4C showed a uniform and dense microstructure (Fig. 10). The presence of boron carbide particles in the coating enhanced the hardness and wear resistance of the material. The surface appeared to be smooth and without any visible cracks or discontinuities, indicating good adhesion and cohesion of the coating. Under high magnification, the surface revealed a uniform distribution of boron carbide particles within the nickel matrix. The particles were well dispersed and did not show any clustering, indicating good mixing and homogeneity. The surface also displayed a high degree of compaction and low porosity, indicating good coating quality [150,151]. The wear surface of the coating after tribological testing showed minimal wear, indicating excellent abrasion resistance (Fig. 10). The surface appeared to be free of any major wear marks, indicating good durability and performance [152]. The wear pattern was also uniform across the surface, indicating that the coating was performing consistently [153,154].

3.5. Corrosion behavior

The corrosion test for the stainless steel-316 has been conducted with 3.5 wt Percent sodium chloride over 120 h. Corrosion weight loss for corroded SS-304 with coating the mixture of Ni and 10% B_4C was found to be 0.42 mg. A Tafel polarization study was also conducted on SS-304 coated with a Ni and 10% B_4C mixture. In this investigation, polished specimens of SS-304 with this coating were immersed in a corrosion medium with varying concentrations of NaOH (0.05 M and 1 M) at an elevated temperature of 300 °C. A stable open circuit potential (OCP) was established. Subsequently, potentiodynamic current-potential curves were generated by polarizing the specimen cathodically to −250 mV and anodically to +250 mV concerning the OCP, with a scan rate of 1 mV s-1. This study aimed to evaluate the material's corrosion behavior and resistance under different conditions, providing insights into its durability and suitability for specific environments. In Fig. 11, potentiodynamic polarization curves for the SS-304 coated with a Ni and 10% B_4C mixture immersed in a NaOH solution at an elevated temperature of 300 °C are depicted. This electrochemical analysis yielded crucial parameters to assess the material's corrosion behavior. Among these parameters were the corrosion rate, cathodic Tafel slope, anodic Tafel slope, corrosion potential, corrosion current density, and corrosion potential. The results revealed a notable correlation between the concentration of NaOH and the corrosion current density. As the NaOH concentration increased, there was a corresponding rise in the corrosion current density [153,154]. This observation suggested that the presence of a more concentrated NaOH solution accelerated the corrosion process of the SS-304 material with the Ni and 10% B_4C coating. Fig. 12 shows the surface morphology of corroded SS-304 with coating the mixture of Ni and 10% B_4C and in which few dark spots may be found. This was because the Ni and B_4C in the coating acted as corrosion inhibitors that provided additional protection to the steel against corrosion. In the presence of a corrosive agent, the Ni and B_4C reacted with the corroding species and formed a protective barrier on the steel surface [153,154]. The morphology of the corrosion varied from simple pitting to more complex forms of corrosion such as crevice corrosion, intergranular corrosion, and selective attack of specific phases [55,58].

However, the corrosion resistance of SS 304 after coating with Ni and B_4C, while improved, faces several limitations and areas for enhancement. Pitting corrosion remains a concern in aggressive environments, necessitating strategies to enhance pitting resistance. Ensuring strong coating-substrate adhesion and minimizing microscopic porosity are critical for long-term stability. Specific corrosion agents require tailored coatings. Thermal cycling can stress the coating, requiring improved thermal stability [153,154]. Addressing cost and scalability concerns is essential for practical industrial adoption. Field testing under real conditions is needed to validate performance, and regulatory compliance must be met. Overcoming these limitations will lead to more robust and versatile corrosion-resistant coatings for SS 304.

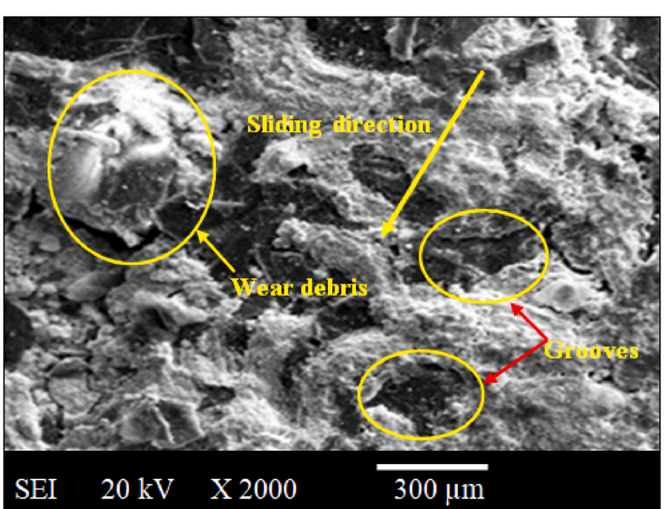

Fig. 10. Wear surface morphology of SS-304 with coating the mixture of Ni and 10% B_4C.

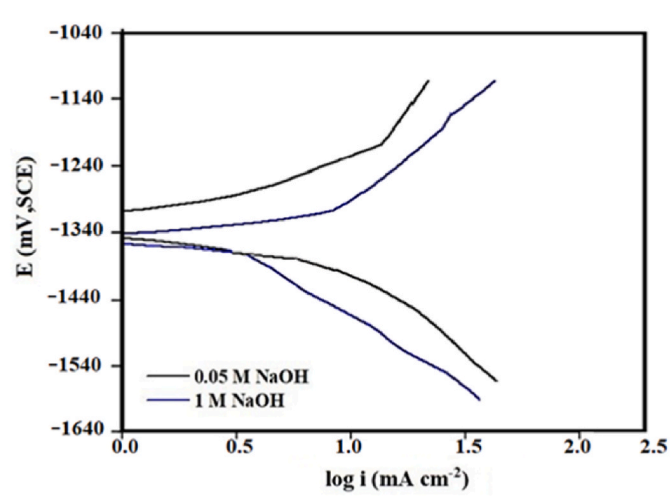

Fig. 11. The Tafel plots for corroded SS-304 with coating the mixture of Ni and 10% B_4C in different concentrations of NaOH at 300 °C.

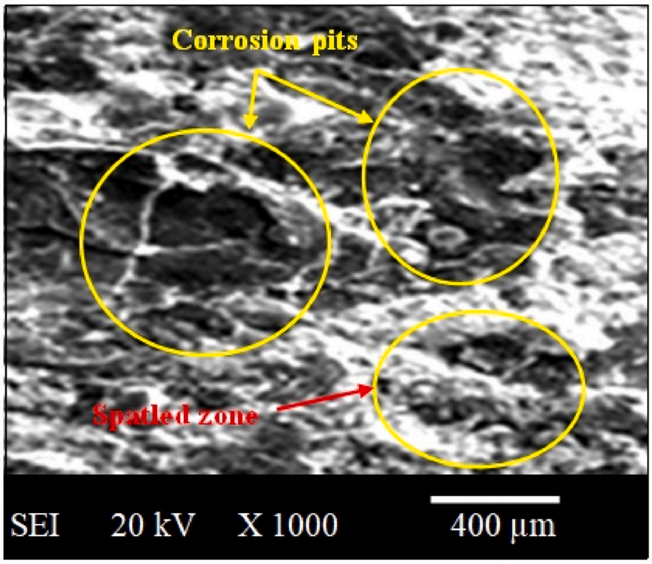

Fig. 12. Surface morphology of corroded SS-304 with coating the mixture of Ni and 10% B_4C.

3.6. Comparison of present study work with previous literature

The present study reported a significant 43.33% enhancement in hardness. This result suggested that the Ni and 10% B_4C coating applied using microwave hybrid heating has effectively improved the hardness of SS-304. Fangyong Niu et al. [33] showed that the microhardness of the TiC ceramic coating on 304 stainless steels reached 654.7 ± 41.0 HV0.2, which was 3.15 times higher compared to WAAM-304. This suggested that the TiC coating significantly enhanced the hardness of the substrate. Abhijit Pattnayak et al. [34] showed that the nano hardness of the Al_2O_3–CeO_2-rGO coating was approximately 87% higher than that of Al2O3–CeO_2 coating. This indicated that the addition of Ceria and reduced graphene oxide significantly enhanced the hardness of the coating. The study of Zhaoliang Li et al. [35] found that when the amount of independent Al_2O_3 was increased to 30%, a strong metallurgical bond developed. This result suggested that the composition of the coating is critical for achieving a strong bond. Shuwei Guo et al. [36] showed that the TiO_2 coating exhibited better protective effects on reducing 316 SS. This indicated that TiO_2 provided improved protection against corrosion in the given environment. Table 3 shows the summary of the comparison of the present study work with previous literature.

4. Conclusions

The microwave cladding technique for depositing Ni and B_4C coatings on 304 stainless steels has yielded significant advancements in various aspects. The key findings and improvements include a remarkable 43.33% enhancement in material hardness, indicative of improved wear resistance and mechanical properties. The uniform distribution of B_4C and Ni on the cladding surface ensured consistent material performance. Microstructural analysis revealed the presence of approximately 2233.35 grains per square inch at 500× magnifications, highlighting the refined grain structure achieved during the cladding process. Wear testing demonstrated a low wear rate of 0.00308 mm^3/m and a favorable coefficient of friction measuring 0.1981, underlining the material's suitability for applications with demanding frictional conditions. Moreover, the corrosion behavior was assessed, revealing a corrosion weight loss of only 0.42 mg for corroded SS-304 with the Ni and 10% B4C coating, indicating notable corrosion resistance. The presence of various carbide phases, including Cr_2C, $Cr_{23}C_6$, Cr_7BC_4, Fe_5C_2, and $Fe_{23}B_6$, within the cladding further contributed to the material's enhanced mechanical and wear properties. Limitations and uncertainties in the findings include potential variations in real-world application conditions, long-term durability, and the need for further environmental testing. Additionally, while microwave cladding shows promise, specific factors affecting material behavior may require more comprehensive investigation for practical industrial implementations. Exploring the future scope for the present study can lead to significant advancements in materials science and engineering. Here are some suggestions for future research and development as In-depth optimization of microwave parameters, such as power, frequency, and exposure time, to further enhance the quality and performance of the coatings; investigation of the thermal behavior of the coatings under various conditions; Investigate the potential benefits of multi-material or multilayer coatings that combine Ni, B4C, and other materials to achieve enhanced properties; Explore the development of nanocomposite coatings. The combination of SS304 with Ni and B_4C coating can be used in the aerospace industry such as including aircraft structural parts and fuel system components. It can be used in the construction of radiation shielding enclosures and containers in nuclear power plants and medical facilities. Coated SS 304 steel with Ni and B_4C may be used in exhaust systems, brackets, and fasteners. It can be also used in boat components, underwater pipelines, and marine hardware.

Ethical approval

Not applicable.

Table 3
Summary of comparison of present study work with previous literature.

S. No.	Ref. No.	Substrate/ Coating Plate	Cladding/Coating Particles	Experimental Set-up	Properties
1	Present Study Work	SS-304	Ni and 10% B_4C	Microwave Hybrid Heating	43.33% enhancement in hardness
2	Fangyong Niu et al. [33]	304 stainless steel	TiC ceramic coating	Wire Arc Additive Manufacturing (WAAM)-Laser Cladding (LC) hybrid	The microhardness of the coating reaches 654.7 ± 41.0 $HV_{0.2}$, which is 3.15 times higher compared to WAAM-304
3	Abhijit Pattnayak et al. [34]	17-4 PH steel	Alumina (Al2O3) doped with 0.8% Ceria (CeO2) and reduced graphene oxide (rGO, 0–0.2%)	High-Velocity Oxygen Fuel (HVOF) thermal spray process	Nano hardness of Al_2O_3–CeO_2-rGO coating is ≈ 87% higher than that of Al_2O_3–CeO_2 coating
4	Zhaoliang Li et al. [35]	Carbon steel	Al_2O_3–TiB_2–TiC ceramic coatings	Laser cladding	When the amount of independent Al_2O_3 was increased to 30%, a strong metallurgical bond developed
5	Shuwei Guo et al. [36]	316 stainless steel	ZrO_2 and TiO_2 ceramic coatings	Air plasma spraying and then exposed to oxygenated sub- and supercritical water	The TiO_2 coating exhibited better protective effects on reducing 316 SS

Consent to participate

Not applicable.

Consent to publish

All authors have read and approved this manuscript.

Author contributions

Conceptualization, SS, SPD,APS, VAS, KAM; methodology, SS, SPD, APS, VAS, KAM; formal analysis, SS, SPD, APS, VAS, KAM; investigation, SS, SPD,APS, VAS, KAM; writing—original draft preparation, SS, SPD, APS, VAS, KAM; writing—review and editing, SS, AK, MIK, MA, EMTE; supervision, SS, AK, MIK, MA, EMTE; project administration, SS, AK, MIK, MA, EMTE; funding acquisition, SS, AK, MIK, MA, EMTE. All authors have read and agreed to the published version of the manuscript.

Data availability statement

The data that support the findings of this study are available within the manuscript.

Funding

The authors extend their appreciation to the Ministry of Education in KSA for funding this research work through the project number KKU-IFP2-DB-6.

Conflict of interests/competing interests

The authors declare no competing interests.

Declaration of interests

The authors declare that they have no known competing financial interests or personal relationships that could have appeared to influence the work reported in this paper.

Acknowledgments

The authors extend their appreciation to the Ministry of Education in KSA for funding this research work through the project number KKU-IFP2-DB-6.

References

[1] Sharma Aman, Chaturvedi Rishabh, Saraswat Manish, Kalra Ravi. Weld reliability characteristics of AISI 304L steels welded with MPAW (micro plasma arc welding). Mater Today Proc 2022;60:1966–72. Part 3.

[2] Kumar Rajeev, Sharma Shubham, Singh Jaiinder Preet, Gulati Piyush, Singh Gursharan, Prakash Dwivedi Shashi, et al. Tag-Eldin, Mohamed Abbas, Enhancement in wear-resistance of 30MNCRB5 boron steel-substrate using HVOF thermal sprayed WC–10%Co–4%Cr coatings: a comprehensive research on microstructural, tribological, and morphological analysis. J Mater Res Technol 2023;27:1072–96.

[3] Singh B, Singh K, Sharma S, et al. Channel engineering assisted performance enhancement of metal gate sub-10nm ballistic SiNWFET for futuristic device applications. Silicon 2022;14:6861–9.

[4] Miniappan Pethampalayam Karuppanan, Marimuthu Sivagnanam, Kumar Selvan Dharani, Gokilakrishnan Gopal, Sharma Shubham, Li Changhe, Dwivedi Shashi Prakash, Abbas Mohamed. Mechanical, fracture-deformation, and tribology behavior of fillers-reinforced sisal fiber composites for lightweight automotive applications. Reviews on Advanced Materials Science 2023;62. 20230342.

[5] Singh Karamvir, Sharma Sandeep, Singh Bhoop, Gupta Monish, Tripathi CC. Fabrication of graphene, graphite and multi wall carbon nano tube based thin films and their potential application as strain sensor. Thin Solid Films 2022;761:139540.

[6] Basanth Kumar Kodli, Sunil B. Ingole, Ali saeedjassim, YatikaGori, Abhishek Kaushik, deepak Kumar, Alok Jain, aluminum-foam by powder metallurgy: a review. Mater Today Proc 2023.

[7] Mohanasundaram S, Bhong Mahesh, Vatsa Ghanshyam, Verma Rajesh Prasad, Srivastava Mahima, Kumar Gaurav, et al. Mg-based metal matrix composite in biomedical applications: a review. Mater Today Proc 2023.

[8] Chandrasekhar B, Dharme Ashwin, Sharma Sachin Kumar, Taluja Resham, Jarali Omkar A, Kalra Ravi. Gaurav Kumar, Role of CNT in influencing the mechanical properties of the Mg-based composites: an overview. Mater Today Proc 2023.

[9] Sambasivam Sangaraju, Gupta Nakul, Jassim Ali Saeed, Singh Durgeshwar Pratap, Kumar Sandeep, Giri Jitendra Mohan, Gupta Manish. A review paper of FSW on dissimilar materials using aluminum. Mater Today Proc 2023.

[10] Lade Jayahari, Mohammed Kahtan A, Singh Devender, Verma Rajesh Prasad, Math Praveen, Saraswat Manish, Gupta Lovi Raj. A critical review of fabrication routes and their effects on mechanical properties of AMMCs. Mater Today Proc 2023.

[11] Sambasivam Sangaraju, Shirbhate Siddheshwar, Abed Ahmed S, Patil Pravin P, Khan Irfan, Singh Rajesh, et al. Significance of reinforcement in Mg-based MMCs for various applications: a review. Mater Today Proc 2023.

[12] Walke Santosh, Kale VM, Patil Pravin P, Giri Jitendra Mohan, Kumar Harish, Kumar Manish, Arun Vanya. Effects of alloying element on the mechanical behavior of Mg-MMCs: a review. Mater Today Proc 2023.

[13] Sambasivam Sangaraju, Abed Ahmed S, Chopde Sushil, Patil Pravin P, Math Praveen, Parmar Ashish, Singh Rajesh, Kansal Lavish, Awasthi Ankita. Role of processing techniques related to Mg-MMCs for biomedical implantation: an overview. Mater Today Proc 2023.

[14] Chaturvedi Rishabh, Sharma Aman, Sharma Kamal, Saraswat Manish. Tribological behaviour of multi-walled carbon nanotubes reinforced AA 7075 nano-composites. Advances in Materials and Processing Technologies 2022;8(4):4743–55.

[15] Sharma Aman, Chaturvedi Rishabh, Sharma Kamal, Saraswat Manish. Force evaluation and machining parameter optimization in milling of aluminium burr composite based on response surface method. Advances in Materials and Processing Technologies 2022;8(4):4073–94.

[16] Keskin Gözde, Salunkhe Sachin, Küçüktürk Gökhan, Pul Muharrem, Gürün Hakan, Baydaroğlu Volkan. Optimization of PMEDM process parameters for B_4C and B_4C+SiC reinforced AA7075 composites. J. Eng. Res. 2023.

[17] Gudipudi Suresh, Nagamuthu Selvaraj, Subbian Kanmani Subbu, Chilakalapalli Surya Prakasa Rao. Enhanced mechanical properties of AA6061-B4C composites developed by a novel ultra-sonic assisted stir casting, Engineering Science and Technology. Int J 2020;23(Issue 5):1233–43.

[18] Dwivedi SP, Yadav AK, Saxena A, Dwivedi VK. Tribo-mechanical, physical and thermal behaviour of Al/Si_3N_4 composite with and without the addition of Cu, Ni and Cr entropy elements. Proc IME E J Process Mech Eng 2023.

[19] Suri Reshal, Nag Tapas C, Mehra Nikita, Neupane Yub Raj, Shafi Sadat, Sharma Devyani, et al. Sirolimus loaded chitosan functionalized PLGA nanoparticles protect against sodium iodate-induced retinal degeneration. J Drug Deliv Sci Technol 2023;82:104369.

[20] Kumar Ajay, Jain Sandeep, Chauhan Shilpi, Aggarwal Shilpy, Saini Deepika. Novel hybrids of quinoline with pyrazolylchalcones as potential antimalarial agents: synthesis, biological evaluation, molecular docking and ADME prediction. Chem Biol Interact 2023;373:110379.

[21] Li Changyuan, Xia Xiaobin, Cai Jun, Zhang Zhihong, Wang Jianhua, Qian Zhicheng, et al. Influence analysis of B4C content on the neutron shielding performance of B_4C/Al. Radiat Phys Chem 2023;204:110684.

[22] Burhan Qader Adnan, Kumar Shobhit, Kohli Kanchan, Abbas Hussein Ahmed. Garlic oil loaded rosuvastatin solid self-nanoemulsifying drug delivery system to improve level of high-density lipoprotein for ameliorating hypertriglyceridemia. Part Sci Technol 2022;40(2):165–81.

[23] Nanda Sanju, Madan Kumud. The role of Safranal and saffron stigma extracts in oxidative stress, diseases and photoaging: a systematic review. Heliyon 2021;7 (Issue 2):e06117.

[24] Wang Shuai, Yang Mingsheng, Li Huaiqian, Wang Luyao, Wang Hong, Xing Pengfei, et al. High-performance B4C matrix composites fabricated from the B4C–Si–CeO2 system via reactive hot pressing. Ceram Int 2022;48(Issue 13):18811–20.

[25] Sheoran M, Sharma R, Chaudhary S, et al. An economical green route synthesis of carbon spheres derived from kitchen biowastes for supercapacitor application. Appl Phys A 2023;129:549.

[26] Kumar Ojha Sanjay, Singh Puneet Kumar, Mishra Snehasish, Pattnaik Ritesh, Dixit Shubha, Verma Suresh K. Response surface methodology based optimization and scale-up production of amylase from a novel bacterial strain, Bacillus aryabhattai KIIT BE-1. Biotechnology Reports 2020;27:e00506.

[27] Li Jiansong, Yang Yang, Gao Qian, Ma Ruina, Fan Yongzhe, An Du, et al. Preparation and characterisation of CeSt3-modified Zn-Ni-B4C composite superhydrophobic coatings. Appl Surf Sci 2023;641:158489.

[28] Radhakrishnan S, Khan A, Dwivedi SP, et al. Studies on mechanical, thermal, and water immersion of plant and animal wastage nanofiller–based bio-fiber-reinforced composites. Biomass Conv Bioref 2023.

[29] Yang Yang, Bian Yi, Gao Qian, Dong Shuhan, Ma Ruina, Fan Yongzhe, et al. Corrosion resistance study of Zn-Ni-B4C composite superhydrophobic coatings with hierarchical rough structure. Appl Surf Sci 2023;622:156882.

[30] Rajkumar G, Saravanan M, Bejaxhin ABH, Sharma S, Dwivedi SP, Kumar R, et al. Parametric optimization of powder-mixed EDM of AA2014/Si3N4/Mg/cenosphere hybrid composites using fuzzy Logic: analysis of mechanical, machining, microstructural, and morphological characterizations. J Compos Sci 2023;7:380.

[31] Sheu Hung-Hua, Wang Qian-You, Lee Ya-Wei. Effects of boron carbide particle content on corrosion resistance and wear resistance of Ni-B/B4C composite coatings. Int J Electrochem Sci 2022;17(Issue 11):221166.
[32] Wei Haoran, Ge Haohui, Zhao Tingting, Sharma Shubham, Petru Michal, Prakash Dwivedi Shashi, et al. Vanadium dioxide thin films-assisted terahertz meta-surface for simultaneous absorption, polarization conversion bi-functional switching, and wavefront operation. Results Phys 2023:106970.
[33] Niu Fangyong, Bi Weiming, Li Cunxu, Sun Xiong, Ma Guangyi, Wu Dongjiang. TiC ceramic coating reinforced 304 stainless steel components fabricated by WAAM-LC integrated hybrid manufacturing. Surf Coating Technol 2023;465:129635.
[34] Pattnayak Abhijit, Gupta Avi, Abhijith NV, Kumar Deepak, Jain Jayant, Chaudhry V. Development of rGO doped alumina-based wear and corrosion resistant ceramic coatings on steel using HVOF thermal spray. Ceram Int 2023;49 (Issue 11):17577–91. Part A.
[35] Li Zhaoliang, Wei Mumeng, Xiao Kui, Bai Ziheng, Xue Wei, Dong Chaofang, et al. Microhardness and wear resistance of Al2O3-TiB2-TiC ceramic coatings on carbon steel fabricated by laser cladding. Ceram Int 2019;45(Issue 1):115–21.
[36] Guo Shuwei, Xu Donghai, Liang Yu, Gong Yanmeng, Li Yanhui, Yang Jianqiao. Corrosion characterization of ZrO2 and TiO2 ceramic coatings via air plasma spraying on 316 stainless steel in oxygenated sub- and supercritical water. J Supercrit Fluids 2020;157:104716.
[37] Jain Pragyan, Sharma Arti, Upadhyay Navya, Tewari Saurabh, Rajput RS, Kumar Sunil, et al. Tribological considerations for failure restoration and maintenance of radial plunger pump against friction and abrasive wear behavior by microwave cladding of Ni-Graphene. Mater Today Proc 2023.
[38] Singh Bhupinder, Zafar Sunny. Microwave cladding for slurry erosion resistance applications: a review. Mater Today Proc 2021;46:2686–90. Part 7.
[39] Durga Prasad C, Shashank Lingappa M, Joladarashi Sharnappa, Ramesh MR, Sachin B. Characterization and sliding wear behavior of CoMoCrSi + Flyash composite cladding processed by microwave irradiation. Mater Today Proc 2021; 46(7):2387–91.
[40] Singh Bhupinder, Zafar Sunny. Understanding time-temperature characteristics in microwave cladding. Manuf Lett 2020;25:75–80.
[41] Vishwanatha JS, Hebbale Ajit M, Kumar Nithin, Srinath MS, Badiger Ravindra I. ANOVA studies and control factors effect analysis of cobalt based microwave clad. Mater Today Proc 2021;46(7):2409–13.
[42] Phanendra Kumar K, Mohanty Aveek, Shashank Lingappa M, Srinath MS, Panigrahi SK. Enhancement of surface properties of austenitic stainless steel by nickel based alloy cladding developed using microwave energy technique. Mater Chem Phys 2020;256:123657.
[43] Singh Bhupinder, Zafar Sunny. Influence of post clad heat treatment on microstructure and slurry erosion characteristics of Ni-based microwave clad. Vacuum 2021;184:109946.
[44] Mishra Tribhuwan Kishore, Kumar Arbind, Sinha SK. Investigation of sliding wear behaviour of Ni-WC microwave cladding. Mater Today Proc 2020;26(2):1418–22.
[45] Babu Abhishek, Arora HS, Singh H, Grewal HS. Microwave synthesized composite claddings with enhanced cavitation erosion resistance. Wear 2019:242–51. Volumes 422–423.
[46] Rakesh B Nair, Arora HS, Boyana AV, Saiteja P, Grewal HS. Tribological behavior of microwave synthesized high entropy alloy claddings. Wear 2019:203028. Volumes 436–437.
[47] Zafar Sunny, Sharma Apurbba Kumar. Structure-property correlations in nanostructured WC–12Co microwave clad. Appl Surf Sci 2016;370:92–101.
[48] Hebbale Ajit M, Srinath MS. Microstructural investigation of Ni based cladding developed on austenitic SS-304 through microwave irradiation. J Mater Res Technol 2016;5(Issue 4):293–301.
[49] Dwivedi SP, Sharma S. Metallic cladding through microwave energy of the mixture of Ni and 15% SiC powder on AISI 304: a green approach in surface engineering. Proc IME E J Process Mech Eng 2023.
[50] Dwivedi SP. Development and characterization of grinding sludge-reinforced aluminum-based composite by friction stir process technique. World Journal of Engineering 2023. ahead-of-print No. ahead-of-print.
[51] Dwivedi S, Selvaprakash S, Sharma S, Kumari Soni, Saxena Kuldeep K, Goyal Rajesh, et al. Evaluation of various properties for spent alumina catalyst and Si3N4 reinforced with PET-based polymer composite. Mech Adv Mater Struct 2023.
[52] Dwivedi S, Sharma S, Vijay Krishna B, Pankaj Sonia, Kumar Saxena Kuldeep, Iqbal Amjad, et al. Effect of the addition of TiB_2 with waste glass powder on microstructure, mechanical and physical behavior of PET-based polymer composite material. Mech Adv Mater Struct 2023.
[53] Dwivedi SP, Chaudhary V, Sharma S, Sharma S. Ultrasonic vibration effect in the development of Al/CCLW/alumina metal matrix composite to enhance mechanical properties. Proc IME E J Process Mech Eng 2023.
[54] Dwivedi SP, Chaudhary V, Sharma S. Effect of the addition of waste glass powder along with TiC as reinforcement on microstructure, wettability, mechanical and tribological behavior of AZ91D magnesium based alloy. Inter Metalcast 2023.
[55] Dwivedi S, Kumar Indradeep, Sehgal Shankar, Gupta Nakul, Kuldeep K, Saxena. Development of dissimilar AA2014 and AA2024 based composite with nano-Si_3N_4 reinforcement by friction stir process technique. J Adhes Sci Technol 2023.
[56] Dwivedi SP, Chaudhary V, Sharma S. Effect of the addition of waste glass powder along with TiC as reinforcement on microstructure, wettability, mechanical and tribological behavior of AZ91D magnesium based alloy. Inter Metalcast 2023.
[57] Dwivedi S, Sharma S, Li C, Zhang Yanbin, Kumar Abhinav, Singh Rajesh, et al. Effect of nano-TiO_2 particles addition on dissimilar AA2024 and AA2014 based composite developed by friction stir process technique. J Mater Res Technol 2023;26:1872–81.
[58] Dwivedi S, Sharma S. Effect of Ni addition on the behavior of dissimilar A356-AZ91/CeO2 aluminum-magnesium based composite fabricated by friction stir process technique. Compos Interfac 2023.
[59] Yu Huan, Luo Zongan, Zhang Xin, Feng Yingying, Xie Guangming. A comparative study of the microstructure and corrosion resistance of Fe-based/B4C composite coatings with Ni-added or Cu-added by vacuum cladding. Mater Lett 2023;335: 133730.
[60] Yu Huan, Luo Zongan, Xie Guangming, Feng Yingying. Effect of Ni additions on microstructure, interfacial diffusion behavior and properties of Fe-based/B4C composite coating by vacuum cladding. Mater Char 2023;196:112491.
[61] Kumar S, Dang R, Manna A, Dhiman NK, Sharma S, Dwivedi SP, et al. Optimization of chemical treatment process parameters for enhancement of mechanical properties of Kenaf fiber-reinforced polylactic acid composites: a comparative study of mechanical, morphological and microstructural analysis. J Mater Res Technol 2023;26:8366–87.
[62] Dwivedi S, Sharma S. Effect of CeO2–Ni addition on the behavior of AZ91- A356 based composite fabricated by friction solid state technique. Mater Chem Phys 2023:128551.
[63] Sharma S, Sudhakara P, Singh Jujhar, Singh Sunpreet, Singh Gurminder. Emerging progressive developments in the fibrous composites for acoustic applications. J Manuf Process 2023;102:443e77. 29 September 2023.
[64] Sharma S, Sudhakara P, Petru M, Singh J, Rajkumar S. Effect of nano- additives on the novel leather fiber/recycled Poly (Ethylene-vinyl-acetate) polymer composites for multifunctional applications: fabrication, characterizations, and multi-objective optimization using Central Composite Design [De Gruyter] Nanotechnol Rev 2022.
[65] Sharma S, Verma A, Rangappa SM, Siengchin S, Ogata S, Recent progressive developments in conductive-fillers based polymer nanocomposites (CFPNC's) and conducting polymeric nanocomposites (CPNC's) for multifaceted sensing applications, J Mater Res Technol, S2238e7854(23)2112-2119.
[66] Lalit Ranakoti, Brijesh Gangil, Kumar Rajesh Pawan, Singh Tej, Sharma S, Li C, et al. Effect of surface treatment and fiber loading on the physical, mechanical, sliding wear, and morphological characteristics of tasar silk fiber waste-epoxy composites for multifaceted biomedical and engineering applications: fabrication and characterizations. J Mater Res Technol JulyeAugust 2022;19:2863e76.
[67] Karthikeyan P, Prabhu L, Bhuvaneswari B, Yokesvaran K, Jerin A, Saravanan R, et al. Influences of various thermal cyclic behaviours on thermo adsorption/ mechanical characteristics of epoxy composite enriched with basalt fiber. Article ID 9716173 Adsorpt Sci Technol 2023.
[68] Sharma Harsh, Kumar Ajay, Rana Sravendra, Gopal Sahoo Nanda, Muhammad Jamil, Rajeev Kumar, et al. Critical review on advancements on the fiber-reinforced composites: role of fiber/matrix modification on the performance of the fibrous composites. J Mater Res Technol 2023;26:2975e3002.
[69] Sharma S, Sudhakara P, Singh Jujhar, Sanjay MR, Siengchin S. Fabrication of novel polymer composites from leather waste fibers and recycled poly(ethylene-vinylacetate) for value-added products. Sustainability 2023;15(5):4333.
[70] Dwivedi SP, S Sharma B, Krishna Vijay, Pankaj Sonia, Kuldeep Kumar Saxena, Iqbal Amjad, et al. Effect of the addition of TiB2 with waste glass powder on microstructure, mechanical and physical behavior of PET-based polymer composite material. Mech Adv Mater Struct 2023:1e10.
[71] Karthik A, Jafrey Daniel James D, Vijayan V, Ahmad Zubair, Rajkumar S, Sharma S, et al. Study on the physicomechanical, fracture-deformation, interface adhesion, and water-absorption properties of twill fabric cotton-bamboo/epoxy composites. J Mater Res Technol 2023.
[72] Miniappan PK, Marimuthu S, Kumar SD, Gokilakrishnan G, Sharma S, Li C, et al. Mechanical, fracture-deformation, and tribology behavior of fillers-reinforced sisal fiber composites for lightweight automotive applications. Rev Adv Mater Sci 2023;62:20230342.
[73] Miniappan PK, Marimuthu S, Dharani Kumar S, Sharma S, Kumar Abhinav, Salah Bashir, Ullah Syed Sajid. Exploring the mechanical, tribological, and morphological characteristics of areca fiber epoxy composites reinforced with various fillers for multifaceted applications. Frontiers in Materials 2023:10.
[74] Rajeev Dhiman, Sharma S, Piyush Gulati, Singh Jai, Jha Kanishka, Chang Li, et al. Fabrication and characterizations of Glass fiber-reinforced functional leaf spring composites with or without microcapsule-based dicyclopentadiene as self-healing agent for automobile industrial applications: comparative analysis. J Mater Res Technol 2023;25.
[75] Teng GAO, Zhang Yanbin, Li C, Wang Yiqi, Yun CHEN, Qinglong AN, et al. Fiber-reinforced composites in milling and grinding: machining bottlenecks and advanced strategies. Front Mech Eng 2022.
[76] Mishra Sandip Kumar, Sanjeev Dahiya, Brijesh Gangil, Lalit Ranakoti, Singh Tej, Sharma S, et al. Mechanical, morphological, and tribological characterization of novel walnut filler reinforced polylactic acid-based biocomposites and prediction based on artificial neural network. Biomass Conversion and Biorefinery; 2022.
[77] Jha Kanishka, Paresh Tamrakar, Rajeev Kumar, Sharma S, Singh Jujhar, Ilyas RA, et al. Effect of hybridization on physiomechanical behavior of vetiver and jute fibres reinforced epoxy composites for structural applications: studies on fabrication, physicomechanical, water-absorption, and morphological properties. J Ind Textil 2022:1e23. SAGE.
[78] Yadav Vikas, Singh Sarbjit, Neeru Chaudhary, Garg Mohinder, Sharma S, Amit Kumar, et al. Dry sliding wear characteristics of natural fibre reinforced poly-lactic acid composites for Engineering applications: fabrication, properties and characterizations. J Mater Res Technol 2023.
[79] Singh Balwant, Raman Kumar, Jasgurpreet Chohan, Sharma S, Singh Jujhar, Ahmad Ilyas, et al. Investigation of copper reinforced Acrylonitrile butadiene

styrene and Nyl on 6 based thermoplastic polymer nanocomposite filaments for 3D Printing of Electro nic Components. High Perform Polym 2022.
[80] Singh Rajawat Abhinay, Singh Sanjeev, Brijesh Gangil, Lalit Ranakoti, Sharma S, Asyraf MRM, et al. Effect of marbles dust on mechanical, morphological, and wear performance of basalt fibre reinforced epoxy composites for structural applications. Polymers 2022;14(7):1325.
[81] Ranakoti L, Gangil B, Mishra SK, Singh T, Sharma S, Ilyas RA, et al. Critical review on polylactic acid: properties, structure, processing, biocomposites, and nanocomposites. Materials 2022;15(12):4312.
[82] Kumar S, Dang R, Manna A, Sharma S, Dwivedi SP, Kumar A, et al. Effect of chemically treated kenaf fiber on the mechanical, morphological, and microstructural characteristics of PLA based sustainable bio-composites fabricated via direct injection molding route. Biomass Conversion and Biorefinery 2023.
[83] Banerjee Abhranil, Jha Kanishka, Petru Michal, Kumar Rajeev, Sharma S, Singh Saini Mandeep, et al. Fabrication and characterization of weld attributes in hot gas welding of alkali treated hybrid flax fiber and pine cone fibers reinforced poly-lactic acid (PLA) based biodegradable polymer composites: studies on mechanical and morphological properties. J Mater Res Technol 2023.
[84] Kumar Raman, Singh Channi Arvinder, Kaur Rupinder, Sharma S, Singh Grewal Jasmaninder, Singh Sehijpal, et al. Exploring the intricacies of machine learning-based optimization of electric discharge machining on squeeze cast TiB2/AA6061 composites: insights from morphological, and microstructural aspects in the surface structure analysis of recast layer formation and worn-out analysis. J Mater Res Technol 2023;26:8569–603. September–October 2023.
[85] Dwivedi S, Sharma S, Sunil BDY, Gupta N, Saxena KK, Eldin SM, et al. Heat treatment behavior of Cr in the form of collagen powder and Al2O3 reinforced aluminum-based composite material. J Mater Res Technol 2023.
[86] Kumar J, Singh D, Kalsi NS, Sharma S, Pruncu CI, Pimenov DY, et al. Comparative study on the mechanical, tribological, morphological and structural properties of vortex casting processed, Al–SiC–Cr hybrid metal matrix composites for high strength wear-resistant applications: fabrication and characterizations. J Mater Res Technol 2020;9:13607–15.
[87] Kumar J, Singh D, Kalsi NS, Sharma S, Mia M, Singh J, et al. Investigation on the mechanical, tribological, morphological and machinability behavior of stir-casted Al/SiC/Mo reinforced MMCs. J Mater Res Technol 2021;12:930–46.
[88] Kumar J, Sharma S, Singh J, Singh S, Singh G. Optimization of wire-EDM process parameters for Al-Mg-0.6Si-0.35Fe/15%RHA/5%Cu hybrid metal matrix composite using TOPSIS: processing and characterizations. J. Manuf. Mater. Process. 2022;6:150.
[89] Garg HK, Sharma S, Kumar R, Manna A, Li C, Mausam K, et al. Multi-objective parametric optimization on the EDM machining of hybrid SiCp/Grp/aluminum nanocomposites using Non-dominating Sorting Genetic Algorithm (NSGA-II): fabrication and microstructural characterizations. Rev Adv Mater Sci 2022;61: 931–53.
[90] Sharma S, Singh J, Gupta MK, Mia M, Dwivedi SP, Saxena A, et al. Investigation on mechanical, tribological and microstructural properties of Al–Mg–Si–T6/SiC/muscovite-hybrid metal-matrix composites for high strength applications. J Mater Res Technol 2021;12:1564–81.
[91] Sharma S, Patyal V, Sudhakara P, Singh J, Petru M, Ilyas RA. Mechanical, morphological, and fracture-deformation behavior of MWCNTs-reinforced (Al–Cu–Mg–T351) alloy cast nanocomposites fabricated by optimized mechanical milling and powder metallurgy techniques. Nanotechnol Rev 2021;11:65–85.
[92] Kumar R, Jha K, Sharma S, Kumar V, Li C, Eldin EMT, et al. Effect of particle size and weight fraction of SiC on the mechanical, tribological, morphological, and structural properties of Al-5.6Zn-2.2Mg-1.3Cu composites using RSM: fabrication, characterization, and modelling. Heliyon 2022;8:e10602.
[93] Muni RN, Singh J, Kumar V, Sharma S, Sudhakara P, Aggarwal V, et al. Multiobjective optimization of EDM parameters for rice husk Ash/Cu/Mg-reinforced hybrid Al-0.7Fe-0.6Si-0.375Cr-0.25Zn metal matrix nanocomposites for engineering applications: fabrication and morphological analysis. J Nanomater 2022;2022:2188705.
[94] Yadav V, Singh S, Chaudhary N, Garg MP, Sharma S, Kumar A, et al. Dry sliding wear characteristics of natural fibre reinforced poly-lactic acid composites for engineering applications: fabrication, properties and characterizations. J Mater Res Technol 2023;23:1189–203.
[95] Yadav V, Singh S, Chaudhary N, Garg MP, Sharma S, Kumar A, et al. Dry sliding wear characteristics of natural fibre reinforced poly-lactic acid composites for engineering applications: fabrication, properties and characterizations. J Mater Res Technol 2023;23:1189–203.
[96] Kumar R, Sharma S, Singh JP, Gulati P, Singh G, Dwivedi SP, et al. Enhancement in wear-resistance of 30MNCRB5 Boron steel-substrate using HVOF thermal sprayed WC-10% Co-4% Cr coatings: a comprehensive research on microstructural, tribological, and morphological analysis. J Mater Res Technol 2023;27(November–December 2023):1072–96.
[97] Singh Yadvinder, Sharma S, Singh Gurpreet, Singh Gursharan, Singh Jujhar, Shashi Dwivedi, et al. Studies on physical, micro-structural, and slurry erosion behaviour of cold sprayed Ni-20CrþTiCþRe coatings on SA516 steel for high-temperature applications. Surf Rev Lett 2023:30.
[98] Dwivedi S, Sharma S, Sharma Kanta Prasad, Kumar Abhinav, Agrawal Ashish, Singh Rajesh, et al. The microstructure and properties of Ni-Si-La2O3 coatings deposited on 304 stainless steel by microwave cladding. Materials 2023;16(6): 2209.
[99] Sundaramali G, Jeeva PA, Karthikeyan S, Kandavel TK, Arulmurugan B, Rajkumar S, et al. Eldin. Experimental investigations of electrodeposited Zn-Ni, Zn-Co, and Ni-CrCo-based novel coatings on AA7075 substrate to ameliorate the mechanical, abrasion, morphological, and corrosion properties for automotive applications. Rev Adv Mater Sci 2023.
[100] Singh Gursharan, Sharma S, Manoj Mittal, Singh Gurminder, Singh Jujhar, Li Changhe, et al. Impact of post-heat treatment on the surface-roughness, residual stresses, and micromorphology characteristics of plasma-sprayed pure hydroxyapatite and 7%-Aloxite reinforced hydroxyapatite coatings deposited on titanium alloy-based biomedical implants [Elsevier] J Mater Res Technol 2022.
[101] Amer Aldawoud, Abdelsalam Aldawoud, Yashar Aryanfar, Haj Assad Mamdouh El, Sharma S, Reza Alayi. Reducing PV soiling and condensation using hydrophobic coating with brush and controllable curtains. Int J Low Carbon Technol 2022;17.
[102] Singh Shailesh Kumar, Somnath Chattopadhyaya, Pramanik Alokesh, Kumar Sanjeev, Shailesh M Pandey, et al. Effect of alumina oxide nano-powder on the wear behaviour of CrN coating against cylinder liner using response surface methodology: processing and characterizations. J Mater Res Technol 2021.
[103] Al-Tameemi, Hamza A, Al-Dulaimi Thamir, Awe Michael O, Sharma S, Pimenov Danil Y, et al. Evaluation of cutting-tool coating on the surface roughness and hole dimensional tolerances during drilling of Al6061-t651 alloy. Materials 2021; 14(7):1783.
[104] Li Haogang, Zhang Yanbin, Li C, Zhou Zongming, Nie Xiaolin, Yun Chen, et al. Extreme pressure and antiwear additives for lubricant: academic insights and Perspectives. Int J Adv Des Manuf Technol 2022.
[105] Singh G, Mittal M, Singh J, Sharma S, Gill AS, Chohan JS, et al. Study on the morphological and mechanical properties of TaC reinforced plasma spray coating deposited on titanium alloy. Mater Today Proc 2022;68:A22e6.
[106] Singh G, Mittal M, Singh J, Sharma S, Chohan JS, Kumar R. Effect of post coating processing on the morphological and mechanical properties of plasma Spray-reinforced hydroxyapatite coating. Mater Today Proc 2022;68:1180e6.
[107] Wang D, Wang X, Jin ML, He P, Zhang S. Molecular level manipulation of charge density for solid-liquid TENG system by proton irradiation. Nano Energy 2022; 103:107819.
[108] Zhang Y, Huang Z, Wang F, Li J, Wang H. Design of bioinspired highly Aligned bamboo-mimetic metamaterials with structural and functional Anisotropy. IEEE Trans Dielectr Electr Insul 2023;30(3):1170–7.
[109] Wang NX, Wang YS, Zheng K, Zhi JQ, Zhou B, Wu YX, et al. Achieving CVD diamond films on Mo0.5(TiZrTaW)0.5 highly concentrated alloy for ultrastrong corrosion resistance. Surf Coating Technol 2023;466:129620.
[110] Liao D, Zhu S, Keshtegar B, Qian G, Wang Q. Probabilistic framework for fatigue life assessment of notched components under size effects. Int J Mech Sci 2020; 181:105685.
[111] Niu X, Zhu S, He J, Liao D, Correia JAFO, Berto F, et al. Defect tolerant fatigue assessment of AM materials: size effect and probabilistic prospects. Int J Fatig 2022;160:106884.
[112] Niu X, Zhu S, He J, Liao D, Correia JAFO, Berto F, et al. Defect tolerant fatigue assessment of AM materials: size effect and probabilistic prospects. Int J Fatig 2022;160:106884.
[113] Deng H, Chen Y, Jia Y, Pang Y, Zhang T, Wang S, et al. Microstructure and mechanical properties of dissimilar NiTi/Ti6Al4V joints via back-heating assisted friction stir welding. J Manuf Process 2021;64:379–91.
[114] Guo K, Gou G, Lv H, Shan M. Jointing of CFRP/5083 aluminum alloy by induction brazing: processing, connecting mechanism, and fatigue performance. Coatings 2022;12(10):1559.
[115] Fu ZH, Yang BJ, Shan ML, Li T, Zhu ZY, Ma CP, et al. Hydrogen embrittlement behavior of SUS301L-MT stainless steel laser-arc hybrid welded joint localized zones. Corrosion Sci 2020;164:108337.
[116] Zhu ZY, Liu YL, Gou GQ, Gao W, Chen J. Effect of heat input on interfacial characterization of the butter joint of hot-rolling CP-Ti/Q235 bimetallic sheets by Laser + CMT. Sci Rep 2021;11(1):10020.
[117] Zhu Q, Chen J, Gou G, Chen H, Li P. Ameliorated longitudinal critically refracted—Attenuation velocity method for welding residual stress measurement. J Mater Process Technol 2017;246:267–75.
[118] Chen Y, Sun S, Zhang T, Zhou X, Li S. Effects of post-weld heat treatment on the microstructure and mechanical properties of laser-welded NiTi/304SS joint with Ni filler. Mater Sci Eng, A 2020;771:138545.
[119] Li H, Si S, Yang K, Mao Z, Sun Y, Cao X, et al. Hexafluoroisopropanol based silk fibroin coatings on AZ31 biometals with enhanced adhesion, corrosion resistance and biocompatibility. Prog Org Coating 2023;184:107881.
[120] Zhao P, Zhu J, Yang K, Li M, Shao G, Lu H, et al. Outstanding wear resistance of plasma sprayed high-entropy monoboride composite coating by inducing phase structural cooperative mechanism. Appl Surf Sci 2023;616:156516.
[121] Wang K, Zhu J, Wang H, Yang K, Zhu Y, Qing Y, et al. Air plasma-sprayed high-entropy (Y0.2Yb0.2Lu0.2Eu0.2Er0.2)3Al5O12 coating with high thermal protection performance. Journal of Advanced Ceramics 2022;11(10):1571–82.
[122] Shi J, Zhao B, He T, Tu L, Lu X, Xu H. Tribology and dynamic characteristics of textured journal-thrust coupled bearing considering thermal and pressure coupled effects. Tribol Int 2023;180:108292.
[123] Ma G, He P, Wang H, Tian H, Zhou L, Yong Q, et al. Promoting bonding strength between internal Al-Si based gradient coating and aluminum alloy cylinder bore by forming homo-epitaxial growth interface. Materials & Design 2023;227: 111764.
[124] Fang JX, Wang JX, Wang YJ, He HT, Zhang DB, Cao Y. Microstructure evolution and deformation behavior during stretching of a compositionally inhomogeneous TWIP-TRIP cantor-like alloy by laser powder deposition. Mater Sci Eng, A 2022; 847:143319.

[125] Dong Y, Shao P, Guo X, Xu B, Yin C, Tan Z. Deformation characterization method of typical double-walled turbine blade structure during casting process. J Iron Steel Res Int 2023.

[126] Lai L, Gan M, Wang J, Chen L, Liang X, Feng J, et al. New class of high-entropy rare-earth niobates with high thermal expansion and oxygen insulation. J Am Ceram Soc 2023.

[127] Hua Y, Li F, Hu N, Fu S. Frictional characteristics of graphene oxide-modified continuous glass fiber reinforced epoxy composite. Compos Sci Technol 2022; 223:109446.

[128] Guo H, Zhang J. Expansion of sandwich tubes with metal foam core under axial compression. J Appl Mech 2023;90(5).

[129] Zhang C, Khorshidi H, Najafi E, Ghasemi M. Fresh, mechanical and microstructural properties of alkali-activated composites incorporating nanomaterials: a comprehensive review. J Clean Prod 2023;384:135390.

[130] Liu M, Huang J, Meng H, Liu C, Chen Z, Yang H, et al. A novel approach to prepare graphite nanoplatelets exfoliated by three-roll milling in phenolic resin for low-carbon MgO-C refractories. J Eur Ceram Soc 2023;43(9):4198–208.

[131] Cao M, Cui T, Yue Y, Li C, Guo X, Jia X, et al. Preparation and characterization for the thermal stability and mechanical property of PLA and PLA/CF samples built by FFF approach. Materials 2023;16(14):5023.

[132] Gao S, Li H, Huang H, Kang R. Grinding and lapping induced surface integrity of silicon wafers and its effect on chemical mechanical polishing. Appl Surf Sci 2022; 599:153982.

[133] Zhang Z, Han Y, Lu X, Zhang T, Bai Y, Ma Q. Effects of N2 content in shielding gas on microstructure and toughness of cold metal transfer and pulse hybrid welded joint for duplex stainless steel. Mater Sci Eng, A 2023;872:144936.

[134] Kuang W, Wang H, Li X, Zhang J, Zhou Q, Zhao Y. Application of the thermodynamic extremal principle to diffusion-controlled phase transformations in Fe-C-X alloys: modeling and applications. Acta Mater 2018;159:16–30.

[135] Zhao Y, Sun Y, Hou H. Core-shell structure nanoprecipitates in Fe-xCu-3.0Mn-1.5Ni-1.5Al alloys: a phase field study. Prog Nat Sci: Mater Int 2022;32(3): 358–68.

[136] Zhao Y, Liu K, Zhang H, Tian X, Jiang Q, Murugadoss V, et al. Dislocation motion in plastic deformation of nano polycrystalline metal materials: a phase field crystal method study. Adv Compos Hybrid Mater 2022;5(3):2546–56.

[137] Zhao Y. Understanding and design of metallic alloys guided by phase-field simulations. npj Comput Mater 2023;9(1):94.

[138] Wang J, Pan Z, Wang Y, Wang L, Su L, Cuiuri D, et al. Evolution of crystallographic orientation, precipitation, phase transformation and mechanical properties realized by enhancing deposition current for dual-wire arc additive manufactured Ni-rich NiTi alloy. Addit Manuf 2020;34:101240.

[139] Zeng L, Lv T, Chen H, Ma T, Fang Z, Shi J. Flow accelerated corrosion of X65 steel gradual contraction pipe in high CO_2 partial pressure environments. Arab J Chem 2023:104935.

[140] Prasanthi Phani, Kumar M, Mallampati Somaiah, Madhav V, Saxena Kuldeep, Mohammed Kahtan, et al. Mechanical properties of carbon fiber reinforced with carbon nanotubes and graphene filled epoxy composites: experimental and numerical investigations. Mater Res Express 2023. 10.

[141] Kumar Rajan, Dwivedi Ravi, Arya Ranjeet, Sonia Pankaj, Yadav Anil, Saxena Kuldeep, et al. Current development of carbide free bainitic and retained austenite on wear resistance in high silicon steel. J Mater Res Technol 2023;24.

[142] Kiranakumar V, Ramakrishnaiah Thejas, Naveen S, Khan M, Gunderi Prasanna, Reddy Sathish, et al. A review on electrical and gas-sensing properties of reduced graphene oxide-metal oxide nanocomposites. Biomass Conversion and Biorefinery 2022.

[143] Shahid Muhammad, Hafiz Muhammad Asif Javed, Ahmad Muhammad, Qureshi Akbar, Khan Muhammad, Alnuwaiser Maha, et al. A brief assessment on recent developments in efficient electrocatalytic nitrogen reduction with 2D non-metallic nanomaterials. Nanomaterials 2022;12.

[144] Singh Bharat, Kumar Indradeep, Saxena Kuldeep, Mohammed Kahtan, Khan M, Ben Moussa Sana, et al. A future prospects and current scenario of aluminium metal matrix composites characteristics. Alex Eng J 2023;76:1–17.

[145] Kumar MS, Sathisha N, Manjnatha S, et al. Fatigue surface analysis of AL A356 alloy reinforced hematite metal matrix composites. Biomass Conv. Bioref. 2023.

[146] Sehar Bakhtawar, Waris Muhammad, Gilani Syed, Ansari Umar, Mushtaq Shafaq, Khan Niaz, et al. The impact of laminations on the mechanical strength of carbon-fiber composites for prosthetic foot fabrication. Crystals 2022;12:1429.

[147] Dikshit MK, Singh S, Pathak VK, Saxena KK, Agrawal MK, Malik V, et al. Surface characteristics optimization of biocompatible Ti6Al4V with RCCD and NSGA II using die sinking EDM. J Mater Res Technol 2023;24:223–35.

[148] Lashin MMA, Ibrahim MZ, Khan MI, Guedri K, Saxena KK, Eldin SM. Fuzzy control modeling to optimize the hardness and geometry of laser cladded Fe-based MG single track on stainless steel substrate prepared at different surface roughness. Micromachines 2022;13(12):2191.

[149] Vemanaboina H, Babu MM, Prerana IC, Gundabattini E, Yelamasetti B, Saxena KK, et al. Evaluation of residual stresses in CO2 laser beam welding of SS316L weldments using FEA. Mater Res Express 2023;10(1):016509.

[150] S Sharma, Xiao Nan Dong, Peng Wei, Chen Long, "Electrochemical deposited Cu-Ni binary and Cu-Ni-Mn ternary alloys from sulphate bath for anti-corrosive coating applications in Brine environment: Effect of Corrosion behaviour, Polarization studies, Morphological and structural characterizations", Key Eng Mater, 837, 102e108. .

[151] Singh Gurbhej, Hitesh Vasudev, Amit Bansal, Sachit Vardhan, Sharma S. Microwave cladding of Inconel-625 on mild steel substrate for corrosion protection. Mater Res Express 2020;7:026512.

[152] Singh J, Gill SS, Dogra M, Singh R, Singh M, Sharma S, et al. State of the art review on the sustainable dry machining of advanced materials for multifaceted engineering applications: progressive advancements and directions for future prospects. Mater Res Express 2022;9(6):064003.

[153] Singh J, Gill SS, Dogra M, Sharma S, Singh M, Dwivedi SP, et al. Effect of ranque-hilsch vortex tube cooling to enhance the surface-topography and tool-wear in sustainable turning of Al-5.6Zn-2.5Mg-1.6Cu-0.23Cr-T6 aerospace alloy. Materials 2022;15(16):5681.

[154] Ganeshkumar S, Singh BK, Kumar SD, Gokulkumar S, Sharma S, Mausam K, et al. Study of wear, stress and vibration characteristics of silicon carbide tool inserts and nano multi-layered titanium nitride-coated cutting tool inserts in turning of SS304 steels. Materials 2022;15:7994.